# Macromolecules

Article

Competitive Copolymerization: Access to Aziridine Copolymers with Adjustable Gradient Strengths

Tassilo Gleede, Jens C. Markwart, Niklas Huber, Elisabeth Rieger, and Frederik R. Wurm*

Max-Planck-Institut für Polymerforschung (MPI-P), Ackermannweg 10, 55128 Mainz, Germany

Ⓢ Supporting Information

ABSTRACT: Competitive copolymerization gives access to gradient copolymers with simple one-step and one-pot strategies. Due to the living nature of the sulfonyl-aziridine polymerization, gradient copolymers can be obtained with low dispersities and adjustable molar masses. The combination of different sulfonyl activating groups allowed to fine-tune the reactivity difference of the comonomers and thus an exact adjustment of the gradient strength. Sulfonyl-activated aziridines are to date the only monomer class providing access to gradient copolymers with reactivity ratios ranging from ($1 \leq r_1 \leq 2$; $1 \geq r_2 \geq 0.5$) for statistical or soft gradient copolymers to block copolymers ($r_1 \geq 20$, $r_2 \leq 0.02$), only by adjusting the electron-withdrawing effect of the activation groups: the reactivity ratios were calculated by different models for a library of eight comonomers. This library was further used to classify between hard, medium, and soft gradients. From the data obtained from the monomer library, it was possible to predict polymerization rate coefficients (k_p) for aziridines, which were not prepared so far: correlation of the shifts in the ^{13}C NMR spectra, the Hammett parameters and secondary parameters such as calculated lowest unoccupied molecular orbital (LUMO) levels of the monomers and the natural charge at the electrophilic carbon, etc., were used to predict (co)monomer reactivity and the resulting gradient strength. We believe that our findings allow us to access tailored gradient copolymers with a controlled monomer sequence distribution depending on the chemical control of comonomer reactivity. With these systematic data on activated aziridines, also more complex copolymer structures can be predicted and prepared. Such materials might find application as linear polyethylenimine derivatives to act as functional polyelectrolytes, or predesigned compatibilizers and surface-active gradient copolymers by a predictable one-step copolymerization.
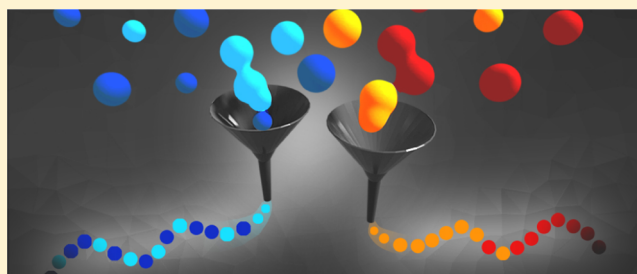
INTRODUCTION

The properties of many biopolymers are defined by their monomer sequence. The precise order of monomers, e.g., nucleotides in our DNA and RNA, contains our genetic code, and the order of amino acids in polypeptides controls the shape of enzymes and thereby determines their activity. Driven by their complex structure, sequence control became a field of research also for artificial polymers, but today's polymer chemistry is still far behind nature's complexity.[1,2] However, also in several synthetic examples, polymer microstructures had a huge impact on material science.[3,4]

Herein, we controlled monomer sequence distribution by a competitive, living copolymerization of monomers with adjustable reactivity that will reflect their positioning along the polymer chain, resulting in adjustable gradient copolymers. Nature uses gradient materials to connect soft and hard tissues or surfaces, such as in bone tissue or nacre.[5] Gradual mineralization or hierarchical pore structures play a crucial role in bioinspired high-performance materials. Squid beaks are a prominent example representing a natural gradient material consisting of chitin and binding proteins, which gradually introduce cross-linking, which causes a hydrophobic environment in the chitin/protein network and a much higher break

modulus and hardness.[6,7] The gradient compared to a discrete section material has the advantage to avoid mechanical mismatches at the interface.[5] Graded mechanical properties also exist in byssal threads of marine mussels, which represent a well-studied underwater adhesive material consisting of protein gradients, which allow fascinating properties regarding adhesive, water resistance, and tensile strength.[8]

In artificial copolymers, gradual monomer incorporation had resulted in unique mechanical properties or self-assembled structures.[9,10] Using the bioinspired principle of gradient materials to produce graded structures and materials is of high interest in orthopedic implants and other high-performance materials.[11] The application of Styrolux and Styroflex as gradient materials and polymer blend compatibilizers shows the impact of using gradient copolymers as additives. Such materials are superior to others in terms of impact strength and toughness of polymer films.[12,13]

Gradient copolymers with different gradient strengths would offer a plethora of possibilities. However, the adjustment of the

gradient strength is difficult to achieve, as often chain-end reactivity is limiting the monomers' compatibility or fixed reactivity ratios result in a single gradient profile only. Continuous monomer addition has been reported to control monomer gradients in controlled radical copolymerization (CRP), but this required precise control over the rate of addition and is thus error-prone.[14−16] To further optimize gradient control in CRP, D'Hooge and co-workers used in silico optimizations to get predetermined feeding strategies based on the Mayo−Lewis equation to achieve a high gradient quality.[17] With atom transfer radical polymerization, they achieved a linear gradient microstructure of *n*-butyl acrylate and methyl methacrylate via a batch approach. Linear gradients in CRP need an appropriate catalytic system, which leads to low dispersities and high monomer conversions.[18] Figure 1A
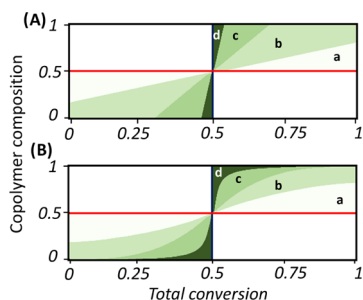

Figure 1. Polymer microstructures of gradient copolymers (of two monomers) with different gradient strengths prepared by living/controlled polymerization: plotted is the copolymer composition of monomer 1, against the total conversion of monomers 1 and 2, for living copolymerizations without termination. (A) Synthesized by continuous monomer feeding, with linear gradients. (B) Synthesized by competitive copolymerization of monomer mixtures with different reactivity ratios, with hyperbolic S-shaped gradient.

illustrates such a graded polymer microstructure obtained using continuous monomer addition, resulting in a typical linear monomer feed. Depending on the speed of monomer addition, copolymers with smooth (area a) or up to hard gradients (area c) can be obtained. In this context, the term "gradient" copolymer is often used for materials with very different gradient profiles. We suggest specifying gradient copolymers according to their gradient profile: soft, medium, hard, and block-like with respect to the differences of their reactivity ratios.

In (competitive) copolymerizations, the gradient strength depends on the reactivity ratios of the individual monomers and their crossover reactions. Reactivity ratios of the comonomers describe the reactivity differences for certain reaction conditions. The comonomer reactivity is chemically fixed and thus should be superior to error-prone dosing techniques. We have studied the anionic copolymerization kinetics for sulfonyl-activated aziridines in recent years and present herein a systematic library of comonomers with precisely adjusted (co)monomer reactivity ratios covering the overall spectrum of gradient strengths (Figure 1B).[19,20] The gradients in Figure 1B can be distinguished from the linear gradients in Figure 1A by its natural S-shape, which can occur symmetrically or asymmetrically. Ganesan used the term "hyperbolic" for gradients prepared by competitive/statistical copolymerizations of monomer mixtures.[21] By the introduction of different sulfonyl activation groups, the (co)monomer's reactivity is controlled, depending on their electron-withdrawing effect (Scheme 1). A combination of different sulfonyl aziridines allows thereby a precise adjustment of the gradient strength in the resulting copolymer. To the best of our knowledge, this is the first example of a comonomer family that allows adjusting the reactivity ratios from perfectly random copolymerization to a formation of block copolymers. If the activating groups are removed after polymerization,[22,23] a full range of gradient polyamines can be prepared. Further combination with epoxides had resulted in a selective copolymerization sequence with access to multiblock copolymers.[24] With this versatile synthesis platform for gradient copolymers with a variable gradient strength, the terminology of "gradient" needs to be specified. With the in situ techniques to follow (co)polymerization reactions, reliable methods to calculate reactivity ratios and polymer microstructures have been developed. From the recorded data, reactivity ratios and Monte Carlo simulations of the comonomer distributions are provided. Monte Carlo simulation as a kinetic model allows illustrating the polymer microstructure. Kinetic models, however, can also determine distributions, chain lengths, and many more features of the copolymers.[25] Due to the systematic data obtained from our monomer library, also the prediction of reactivity ratios by Hammett parameters or the ^{13}C NMR shift of monomers was feasible. These easy design principles will allow the preparation of functional poly(sulfonyl-aziridine)s or (after hydrolysis) polyamines for various applications.[22,23]

Scheme 1. Synthesis of Sulfonyl-Activated Aziridines Starting from 2-Methyl Aziridine and Sulfonyl Chlorides (1−8)[a]
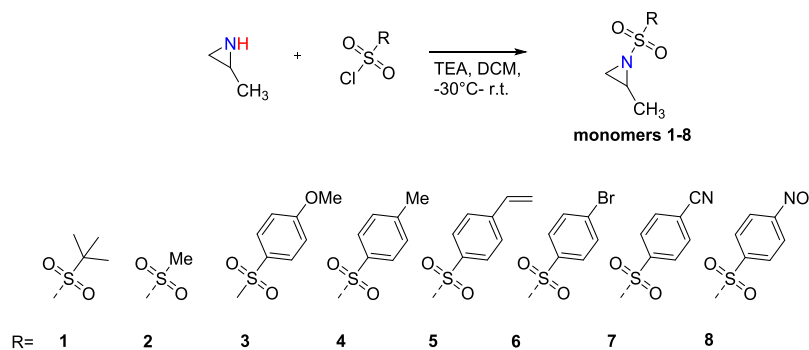
[a]The monomers are sorted by increasing the electron-withdrawing effect of the activation group (AG). TEA = triethylamine, DCM = dichloromethane.

Table 1. Relative ^{13}C NMR Shifts and Hammett Parameters for Monomers 1−8 and Kinetic Data and Molar Mass Characteristics of P1−P8[a]

monomer	(1)[a]	(2)[a]	(3)	(4)	(5)[b]	(6)[c]	(7)	(8)[c]
refs	[20]	[20]	this work	[20]	[29]	[20]	this work	[20]
C_2−^{13}C NMR shift	34.03	35.13	35.75	35.85	36.03	36.26	36.70	36.84
Hammett parameter σ			−0.27	−0.17	−0.04	0.23	0.66	0.78
$k_p/10^{-3}$ L mol^{-1} s^{-1}	5	15	37	41	50	71	90	97

[a]Calibration to solvent signal (77.16 ppm). [b]k_p value of **5** was determined via a correlation method using eq 15. [c]k_p values were taken from the literature. Polymerizations conducted with a 10 wt % monomer concentration, with 50 equiv. monomer to 1 equiv. initiator at 50 °C in DMF-d_7.

■ EXPERIMENTAL SECTION

Materials. All solvents and reagents were purchased from Sigma-Aldrich, Acros Organics, or Fluka and used as received unless otherwise mentioned. All deuterated solvents were purchased from Deutero GmbH and distilled from CaH$_2$ or sodium and stored in a glovebox prior to use. All monomers and initiators were dried extensively by azeotropic distillation with benzene prior to polymerization. 2-Decyl-N-busyl-aziridine (**1**) was synthesized according to previous protocols.[18] 2-Methyl-N-mesyl-aziridine (**2**), 2-methyl-N-tosylaziridine (**4**), 2-methyl-N-brosylaziridine (**6**), 2-methyl-N-nosylaziridine (**8**), and N-benzyl methane sulfonamide (BnNHMs) were synthesized to our previously published protocol.[26] 2-Decyl-N-mesyl-aziridine and 2-decyl-N-tosyl-aziridine were synthesized according to a previously published protocol.[27,28] **5** was synthesized according to the literature.[29] 2-Methyl-N-(4-methoxyphenyl)sulfonyl-aziridine (**3**) and 2-methyl-N-(4-cyanophenyl)sulfonyl-aziridine (**7**) were synthesized in analogy to **4** (analytical details below and ^{1}H NMR, ^{13}C NMR in the Supporting Information Section 3).

Instrumentation. NMR: ^{1}H NMR spectra were recorded using a Bruker Avance 300, a Bruker Avance III 700. All spectra were referenced internally to residual proton or carbon signals of the deuterated solvent, if not noted otherwise.

SEC: size exclusion chromatography (SEC) measurements of polymers were performed in dimethylformamide (DMF) either at 60 °C and a flow rate of 1 mL/min with a PSS SECcurity as an integrated instrument (1 g L^{-1} LiBr added) with a PSS GRAM 100−1000 column and a refractive index (RI) detector or in DMF (containing 0.25 g L^{-1} LiBr) on an Agilent 1100 Series as an integrated instrument, including a PSS HEMA column ($10^6/10^5/10^4$ g mol^{-1}) and an RI detector at a flow rate of 1 mL min^{-1} at 50 °C. Calibration was carried out using poly(ethylene glycol) standards provided by Polymer Standards Service.

Synthesis of 7. In a dry 250 mL, round-bottom flask equipped with a stirring bar, 4-cyanobenzolsulfonylchloride (7.5 g, 36 mmol) was dissolved in 200 mL of dry dichloromethane. The reaction mixture was cooled in a dry-ice acetone bath at −30 °C. Triethylamine (4.5 mL, 3.3 g, 33 mmol) was added slowly via a syringe. Freshly distilled methyl aziridine (2.4 mL, 33 mmol) diluted in 20 mL of dry dichloromethane was added dropwise to the reaction mixture. After stirring for 30 min at −30 °C, the reaction mixture was further stirred at room temperature for 2 h. The dichloromethane (DCM) phase was washed with water (3 × 50 mL), 0.2 N HCl (1 × 50 mL), saturated sodium bicarbonate solution (1 × 50 mL), and brine (1 × 50 mL). The organic layer was dried over MgSO$_4$, filtered, and concentrated below 30 °C at reduced pressure to give the product as a colorless solid (yield: 6.8 g, 93%). Polymerizations were conducted with freshly recrystallized monomer. Therefore, the monomer was dissolved in *tert*-butyl methyl ether (1 g in 2 mL) and recrystallized at −20 °C (small amounts of petroleum ether can be added if not crystallization occurs under these conditions); yield 400 mg (40%) purified monomer. Note: the supernatant after recrystallization can be concentrated at reduced pressure, and recrystallization can be performed again. Attempted purification by sublimation or column chromatography over silica indicated a ring-opened product.

^{1}H NMR (300 MHz, benzene-d_6) δ 7.66−7.47 (m, 2H), 6.88−6.70 (m, 2H), 2.53 (h, J = 5.7 Hz, 1H), 2.24 (dd, J = 7.0, 1.6 Hz, 1H), 1.34 (dd, J = 4.6, 1.6 Hz, 1H), 0.71 (dd, J = 5.6, 1.6 Hz, 3H).

^{13}C NMR (176 MHz, chloroform-d) δ 142.92, 132.99, 128.52, 117.32, 36.82, 35.56, 16.90.

Synthesis of 3. In a dry 100 mL, round-bottom flask equipped with a stirring bar, 4-methoxybenzolsulfonylchloride (3.0 g, 14.4 mmol, 1 equiv) was dissolved in 70 mL of dry dichloromethane. The reaction mixture was cooled in a dry-ice acetone bath at −30 °C. Triethylamine (3 mL, 21 mmol, 1.5 equiv) was added slowly via a syringe. Freshly distilled methyl aziridine (1.0 mL, 16 mmol, 1.1 equiv) diluted in 20 mL of dry dichloromethane was added dropwise to the reaction mixture. After stirring for 30 min at −30 °C, the reaction mixture was further stirred at room temperature for 2 h. The DCM phase was washed with water (3 × 50 mL), saturated sodium bicarbonate solution (1 × 50 mL), and brine (1 × 50 mL). The organic layer was then dried over MgSO$_4$, filtered, and the solvent was removed at reduced pressure (yield: 2.5 g, 83%). Further purification by column chromatography over silica can be conducted with petrol ether and ethyl acetate (3:7 volume ratio) R_f: 5.4. The product was obtained as a colorless solid.

^{1}H NMR (300 MHz, chloroform-d) δ 7.94−7.82 (d, 2H), 7.05−6.96 (d, 2H), 3.88 (s, 3H), 2.88−2.72 (m, 1H), 2.59 (d, J = 7.0 Hz, 1H), 2.01 (d, J = 4.6 Hz, 1H), 1.25 (d, J = 5.6 Hz, 3H).

^{13}C NMR (75 MHz, chloroform-d) δ 163.68, 130.11, 130.00, 118.30, 114.40, 55.79, 35.92, 34.84, 16.94.

Monitoring Polymerizations by In Situ ^{1}H NMR Spectroscopy. Inside of a glovebox in a nitrogen atmosphere, 100 mg of the respective monomer or monomer mixture was dissolved as a 10 wt % solution with a total volume of 1.0 mL of deuterated DMF. A monomer-to-initiator ratio of $[M]_0/[I]_0 = 50{:}1$ was used in all cases. The initiator solution in 1 mL of deuterated DMF was prepared separately, e.g. BnNHMs (10 equiv) and potassium bis-(trimethylsilyl)-amide (KHMDS) (10 equiv) in 1 mL of DMF-d_7. From this, 1/10th (1 equiv) was used. A conventional NMR tube was filled with the monomer(s) in DMF and sealed with a rubber septum. From the initiator stock solution, 100 µL was added to the monomer mixture, mixed quickly, and inserted into the spectrometer. All ^{1}H NMR kinetics were recorded using a Bruker Avance III 700. All spectra were referenced internally to residual proton signals of the deuterated solvent dimethylformamide-d_7 at 8.03 ppm. The $\pi/2$-pulse for the proton measurements was 13.1 µs. The spectra of the polymerizations were recorded at 700 MHz with 32 scans (equal to 404 s (acquisition time of 2.595 s and a relaxation time of 10 s after every pulse)) until the polymerization was completed. No B-field optimizing routine was used over the kinetic measurement time. The spin−lattice relaxation rate (T1) of the ring protons, which are used afterward for integration, was measured before the kinetic run with the inversion recovery method.[30]

Determination of Reactivity Ratios. The reactivity ratios illustrated in Table 1 were calculated by three different nonterminal models following the instructions of Jaacks,[36] Frey,[32] or BSL[33] and the Meyer−Lowry[34] model as a terminal model. For the anionic polymerization of aziridines, a nonterminal approach should be valid, given our previous studies: the propagating sulfonamide anions do not differ significantly in their size or nucleophilicity,[35] indicating a similar chain-end reactivity for all growing chains. We further assume efficient initiation by the activated initiator because the sulfonamide initiator (BnNHMs) is fully deprotonated.

Calculation of reactivity ratios using the Jaacks model:

Scheme 2. Living Anionic Ring-Opening Polymerization of Activated Aziridines (AG = Activation Group)
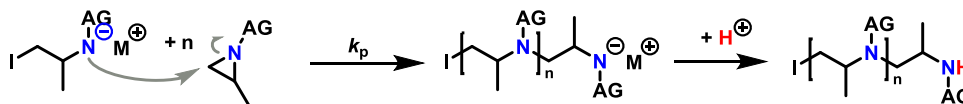
The Jaacks model estimates the reactivity ratios under the assumption of an ideal copolymerization $r_1 \times r_2 = 1$.[36] Using this assumption, the following equation can be used to fit the experimental data.[36]

Copolymerization equation of an ideal copolymerization[36]

$$\frac{d[M_1]}{d[M_2]} = r_1 \frac{[M_1]}{[M_2]} \tag{1}$$

$$\frac{[M_1]}{[M_{1,0}]} = \left(\frac{[M_2]}{[M_{2,0}]}\right)^{r_1} \tag{2}$$

$$\log\left(\frac{[M_1]}{[M_{1,0}]}\right) = r_1 \log\left(\frac{[M_2]}{[M_{2,0}]}\right) \tag{3}$$

$$r_2 = \frac{1}{r_1} \tag{4}$$

Calculation of reactivity ratios using the Meyer–Lowry model[34]

$$X = 1 - \left(\frac{f}{f_0}\right)^{r_2/1-r_2} \times \left(\frac{1-f}{1-f_0}\right)^{r_1/1-r_1}$$
$$\times \left(\frac{f - \frac{1-r_2}{2-r_1-r_2}}{f_0 - \frac{1-r_2}{2-r_1-r_2}}\right)^{r_1 r_1 - 1/(1-r_1)(1-r_2)} \tag{5}$$

Calculation of reactivity ratios using the Frey model:[32]

The ideal integrated model estimated the reactivity ratios under the assumption of a simplified version of an ideal copolymerization and defined $r_1 \times r_2 = 1$. This model is mathematically less complex and prevents overfitting. r_2 is calculated with eq 4 and not by fitting. Eq 6 is similar to the first two terms of the Meyer–Lowry equation. However, the exponents, containing the reactivity ratios, only consider a single r-value as its origin is a nonterminal ideal model ($r_2 \times r_2 = 1$).

$$X = 1 - \left(\frac{f}{f_0}\right)^{1/r_1-1} \times \left(\frac{1-f}{1-f_0}\right)^{r_1/1-r_1} \tag{6}$$

Calculation of reactivity ratios using the BSL model:

The BSL model is another nonterminal model for the calculation of the reactivity ratios, using the following definition for the monomer conversion using eqs 7 and 8 from the literature.[33] The equation enables the determination of reactivity ratios at any conversion for copolymerizations, which follow the nonterminal model of copolymerization kinetics

$$X = 1 - f_{1,0}\left(\frac{M_1}{M_{1,0}}\right) - (1-f_{1,0})\left(\frac{M_1}{M_{1,0}}\right)^{r_2} \tag{7}$$

$$X = 1 - f_{1,0}\left(\frac{M_2}{M_{2,0}}\right)^{r_1} - (1-f_{1,0})\left(\frac{M_2}{M_{2,0}}\right) \tag{8}$$

Calculation of the Copolymer Microstructure. The copolymer microstructure can be calculated by the previously obtained reactivity ratios r_1 and r_2. Therefore, the instantaneous copolymer composition F_1 is plotted against the total monomer conversion X.

Equations used for the calculation of the copolymer microstructure

$$X = 1 - \frac{[M_1] + [M_2]}{[M_{1,0}] + [M_{2,0}]} \tag{9}$$

$$b = \frac{[M_1]}{[M_2]} \tag{10}$$

$$\varepsilon = \frac{1 + r_1 b}{1 + r_2 b^{-1}} \tag{11}$$

$$F_1 = \frac{\varepsilon}{1 + \varepsilon} \tag{12}$$

■ COMPUTATIONAL DETAILS

All density functional theory (DFT) calculations were carried out with the Gaussian 09 package.[37] The structures were optimized at the B3LYP level of theory,[38] with the basis set of 6-31+G*.[39,40] Accurate electronic energies were obtained from single point calculations at the B3LYP level upon the optimized structures, in conjunction with the 6-311++G** basis set.[39,41] The single point calculations were performed together with the polarizable continuum model (PCM) by employing DMF as the solvent.[42–44] Vertical ionization potentials and electron affinities were computed with the solution-phase single point electronic energies. Population analysis was carried out using the natural bond orbital option within the single point calculations.[45]

The following equations have been used to calculate the interested properties

$$\mu = -\frac{1}{2}(\text{IP} + \text{EA}) \tag{13}$$

$$\eta = \text{IP} - \text{EA} \tag{14}$$

where IP is the ionization potential, EA is the electron affinity, η is the chemical potential, and μ is the chemical hardness. The IP and EA were calculated based on the relax geometries of cations and anions.

■ RESULTS AND DISCUSSION

To synthesize gradient copolymers in a batch or one-pot reaction, it is essential to use a controlled or living polymerization techniques. Living anionic polymerization of aziridines was conducted in 2005 for the first time by substituting the *N*-proton with a sulfonyl group(Scheme 2).[46] The electron-withdrawing nature of the sulfonyl group allows a nucleophilic attack on the nonsubstituted side of the aziridine ring. Depending on the electron-withdrawing strength of the sulfonyl substituents, the monomer reactivity can be adjusted.[20] By choosing functional groups either as a side group in the 2-position[27,47] or on the activation group,[29] multiple functional polyethylenimine derivatives are accessible.

We previously studied the polymerization kinetics of activated aziridines under different conditions. In contrast to epoxide polymerization, different alkali metal counterions only slightly influenced the polymerization kinetics;[48] the presence of protic impurities is tolerated by the weakly basic sulfonamide chain end but slowed down propagation rates.[35]

Multigradient copolymers had been prepared by copolymerization of up to five different activated aziridines in solution[20] or adjustable gradient copolymers were prepared by polymerization in emulsion.[28]

Monomer Synthesis and Polymerization. Monomers **1**, **2**, **4−6**, and **8** were prepared according to our previous protocols.[20,29,46] **3** and **7** were synthesized to enlarge the comonomer reactivity library by a similar protocol: the one-step reaction of 2-methyl aziridine and the respective sulfonyl chlorides was applied with yields higher than 80% in most cases.[20,29,46] Both the novel monomer **7** and monomer **8**[20] are highly reactive to moisture, and special care has to be taken in their purification and storage (see Experimental Section for details). Similar findings were reported by Rupar and co-workers for other nitrosyl aziridines.[49] To suppress spontaneous polymerization of **7** or **8**, it proved to be essential to remain the temperatures below 30 °C during workup and to use mild recrystallization for purification. The polymerizations were conducted in an NMR tube, resulting in well-defined polysulfonamides with narrow molar mass distributions and monomodal SEC elugrams (representative examples for P(3) and P(7) are reported in Figures S15 and S17).

Prediction of the Monomer Reactivity and a Forecast on the Polymer Microstructure. The electron-withdrawing (EWD) behavior of the sulfonyl groups in the monomer library (**1−8**) was quantified (Scheme 1): to predict comonomer gradient profiles, the ^{13}C NMR shifts of the ring carbons can be used easily to illustrate the electron-withdrawing strength of the different sulfonamides. Figure 2A shows a zoom into the ^{13}C NMR spectra of the monomers. For a better comparison between the different electron-withdrawing groups, the

chemical shift of the pendant methyl group was set as a reference. The relative chemical shifts of the electrophilic carbons in the 2- and 3-positions clearly shifted downfield, with increasing EWD strength of the substituents from **1** to **8**. The Hammett parameter (σ), a substituent constant correlating originally to the reaction coefficient of benzoic acid derivatives, also correlates with the carbon shift of the ^{13}C NMR spectra, allowing to quantify and to predict the copolymerization behavior. Figure 2B illustrates the relation of the Hammett parameter of each monomer with the chemical shifts determined from the ^{13}C NMR spectra. A similar linear relation of the Hammett parameter with the β-carbon shifts of different vinyl monomers was reported by Ishizone et al.[50] We here observed this trend for monomers, which undergo ring-opening polymerization; to the best of our knowledge, a similar reactivity profile has not been reported for oxiranes, thiiranes, cyclic esters, or other cyclic monomers for ring-opening polymerization.

The propagation rate coefficient (k_p) for the polymerizations of monomers **1−8** (except **5**) was determined from in situ ^{1}H NMR spectroscopy by a previously reported method.[20] The k_p-values correspond to the electron-withdrawing effect of the sulfonyl group in the orders **1** (slow) to **8** (fast); ^{1}H NMR data for the new P3 and P7 are summarized in Figures S16 and S18. Table 1 summarizes the kinetic data for the polymerizations, the ^{13}C NMR shifts, and the Hammett parameters (σ) for all monomers. Section 3 in the Supporting Information summarizes the theoretical and experimental molar masses and the dispersities (determined by SEC). The apparent molar masses from SEC of polyaziridines (e.g., **3** and **7**) are underestimated compared to the theoretical molar mass on our setup, which might be attributed to the hydrophobic character of the polymers. Also, the relatively high molar mass of the pendant chains does not increase the hydrodynamic radii of the polymers, which further decreases the apparent molar masses in SEC.

Besides the ^{13}C NMR shift of each monomer, also the propagation rate coefficient (k_p) correlated in the same trend to the Hammett parameters (Figure 3; note: monomers having a nonaromatic activation group (**1** and **2**) are shown in gray, not included in the fit). Based on the ^{13}C NMR shifts and/or the Hammett parameters, the prediction of the propagation rates of other activated aziridines becomes feasible by the following fit equations calculated from the experimental data (from Figure 3A,B)

$$k_p = 58 \times \sigma + 52 \tag{15}$$

$$k_p = 56 \times {}^{13}\text{C shift} - 1973 \tag{16}$$

The k_p value for monomer **5** was calculated exemplarily: eq 15 gave $k_p = 50 \times 10^{-3}$ L mol^{-1} s^{-1}, while eq 16 gave a very similar $k_p = 52 \times 10^{-3}$ L mol^{-1} s^{-1}, indicating that both relations can be used to estimate polymerization kinetics, which corresponded well with its copolymerization behavior (cf. Table 3). Figure 4 shows several predicted values for aromatic sulfonyl-activated aziridines based on the Hammett parameters of the substituents (Table S1 summarizes the Hammett parameters according to reference[51] and the calculated k_p values according to eq 15. Note: the Hammett parameters are only valid for aromatic sulfonamides; the aliphatic sulfonamides, however, seem to follow the same trend of reactivity controlled by the EWD of the respective group).
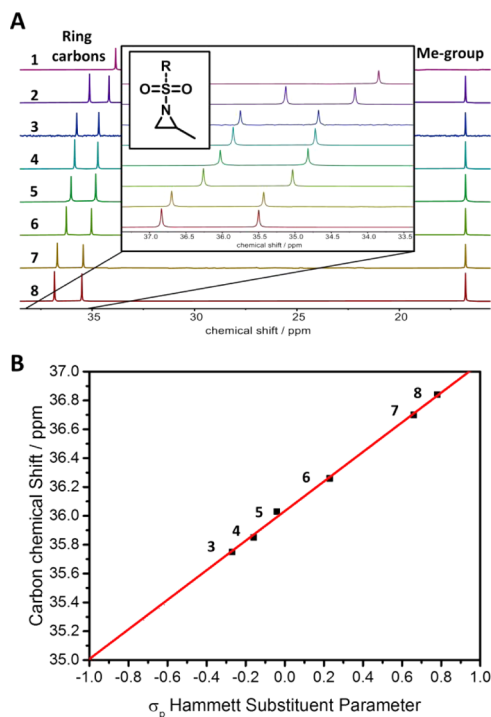

Figure 2. (A) Zoom into the ^{13}C NMR spectra of activated aziridines **1−8** ordered from top to bottom with increasing EWD behavior (note: the chemical shift of the pendant methyl group was used as a reference), and (B) correlation between the ^{13}C NMR shift and the Hammett substituent parameter σ. (Note: values for monomers 1 and 2 are not listed, as they carry aliphatic sulfonamides.)
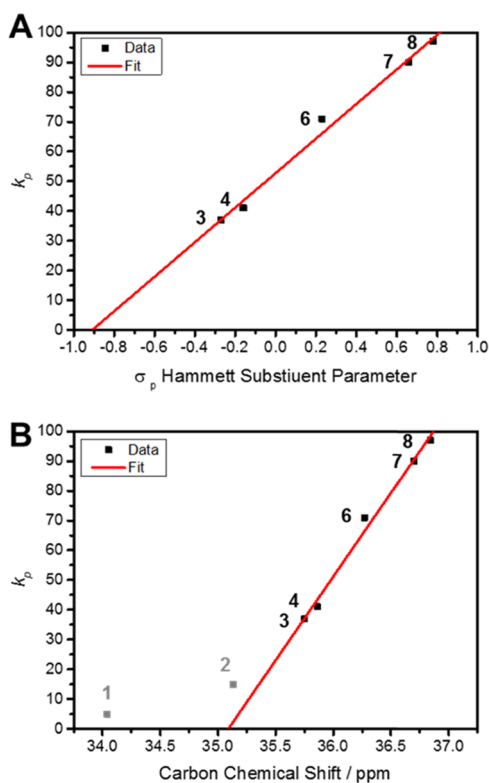
Figure 3. (A) Correlation between the determined k_p values and the Hammett substituent parameter. (B) Correlation between k_p values and ^{13}C shift of the 3-positioned ring carbon (in gray, the aliphatic activation groups, excluded from the linear fit).
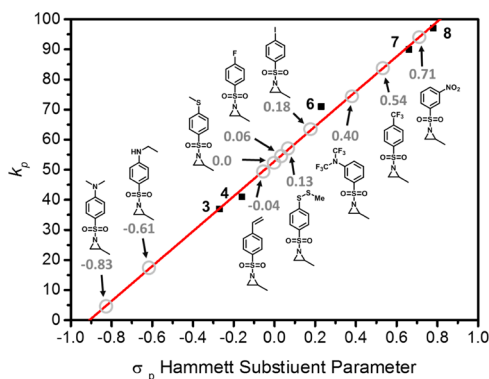

Figure 4. Prediction of propagation rate coefficient (k_p) of various sulfonyl aziridines vs. Hammett parameters (black squares: measured, gray circles: Hammett parameters are taken from the literature and estimated k_p value).

In addition to NMR data and Hammett parameters, DFT calculations were conducted to quantify the electron-withdrawing behavior and correlate this to the monomer reactivity. Calculations were performed employing the Gaussian self-consistent reaction field (SCRF) option with *N,N*-dimethylformamide as the solvent. Details on this option can be found here, https://gaussian.com/scrf/, and details on the overall setup of the calculations are provided in the Computational Details section. To assess the monomers' reactivity, lowest unoccupied molecular orbital (LUMO) and highest occupied molecular orbital (HOMO) energies of the sulfonyl aziridines, bond lengths of the N−S bond, and the natural charge of the electrophilic site of the activated aziridines were used (cf.

Table S2). In all cases, also, these calculated values allow sorting sulfonyl-activated aziridines to their expected ^{13}C NMR shifts or propagation rates (Figure S1). Figure S1A shows the LUMO and HOMO energies of all monomers. As LUMO energies decrease with increasing EWD, this calculation allows a quick estimation of monomer reactivity. The data indicated that a potential monomer with a reactivity higher than monomer **8** has a LUMO energy, which is lower than −3.5 eV and thereby probably very unstable and plagued by spontaneous polymerization. The nitrosyl monomers prepared by Rupar et al.[49] are an example of such highly reactive sulfonyl aziridines as they spontaneously ring-opened. Such findings are supported by the data from Stanetty and co-workers, who reported on dinosyl-activated aziridines that ring-opened rapidly in the presence of alcohols.[52] As Figure S1B,D illustrates, the N−S bond distance shortens systematically, which correlates with the explanations that the free electron pair of the nitrogen compensated the electron loss on the sulfur caused by the activation group. The natural charge at the electropositive carbon in Figure S1C,E represents the electrophilicity of the 3-positioned carbon caused by the EWD nature of the activation groups, with very reactive monomers having a higher natural charge. In summary, sulfonyl-activated aziridines allow a systematic adjustment of comonomer reactivity and thus the preparation of a variety of gradient copolymers.

Copolymers: Reactivity Ratios and Variation of Polymer Gradient Strength. The monomer sequence distribution in the copolymers of sulfonyl aziridines depends on the different EWD group of each comonomers. Hoogenboom and co-workers recently studied cationic ring-opening copolymerizations of oxazolines and oxazines and reported that the reactivity ratios depended on the nucleophilicity of the monomers and less on the electrophilicity of the chain end.[53,54] For anionic polymerization, the comonomer reactivity depends mostly on the electrophilic nature of the monomers but not on the nucleophilicity of the active chain end.[35] Copolymers with different gradient profiles had been reported from carbanionic,[55−57] oxyanionic,[32,58] and azaanionic copolymerization.[20,28] In general, reactivity ratios can be calculated from copolymerization data via different models. The oldest methods to extract reactivity ratios were developed by Wall,[31] followed by Alfrey and Goldfinger,[59] as well as Mayo and Lewis.[60] They can be used for either terminal or nonterminal polymerizations. However, the differential equations are replaced by modern integrated fitting models. Meyer and Lowry applied an integrated Mayo−Lewis equation. The Meyer−Lowry model can directly fit the experimental data: comonomer composition (*f*) in the reaction mixture depending on the total comonomer conversion (*X*) in the form of a compositional drift.[34] Meyer−Lowry and other integrated models are further distinguished by being nonterminal or terminal models, meaning that the nature of the active chain end has or has no effect on the polymerization. Modern in silico modeling techniques can also consider the influence of the monomer sequence just before the active chain end, e.g., two monomers (penultimate), three monomers (penpenultimate).[25,61]

Reactivity ratios were calculated by nonterminal models. Recently, Lynd and co-workers suggested that reliable reactivity ratios could be calculated either via the Meyer−Lowry (if the terminal model is required) or the Beckingham−Sanoja−Lynd method (BSL/nonterminal model) because the integrated methods are more accurate than linearized models.
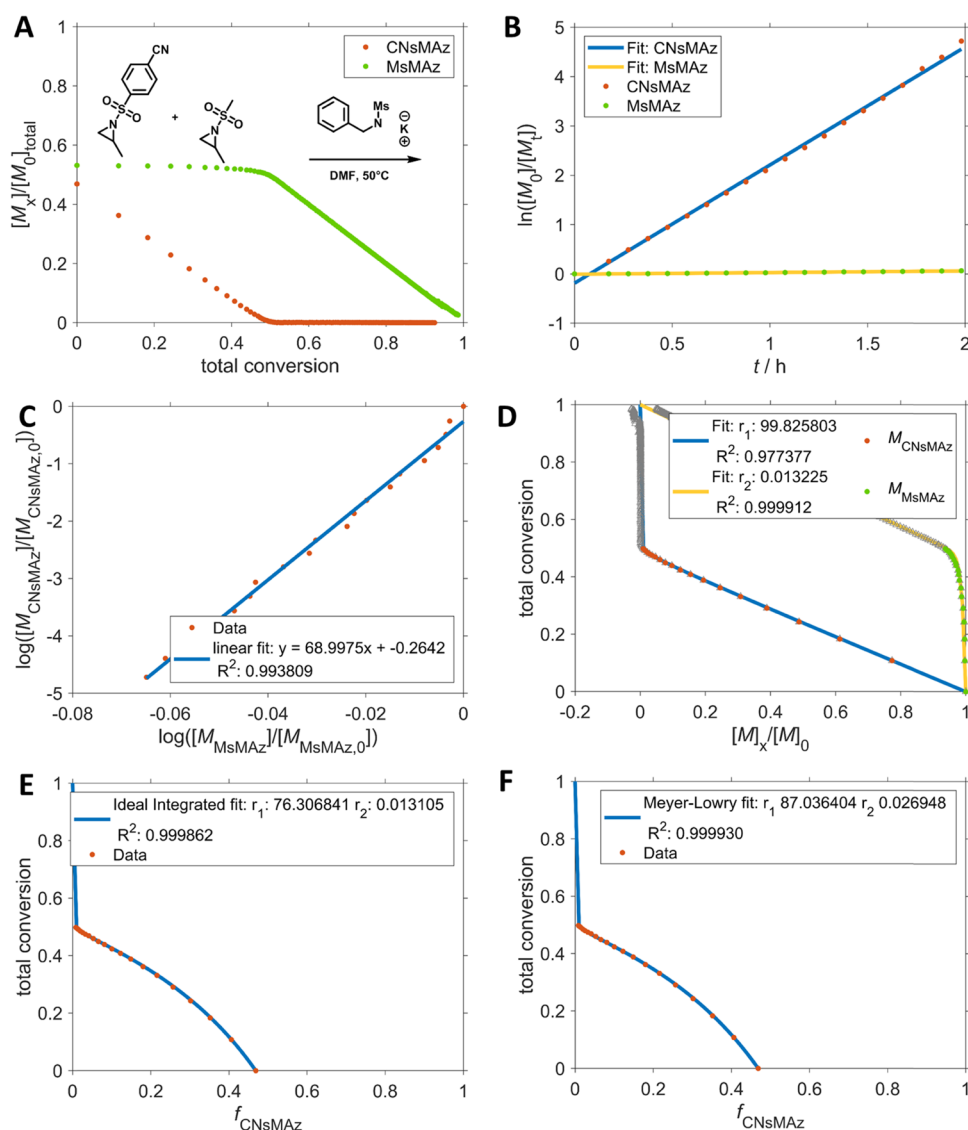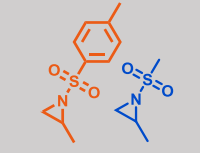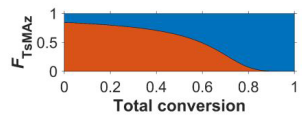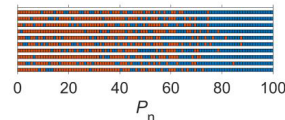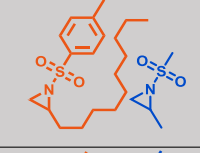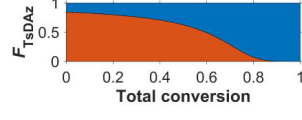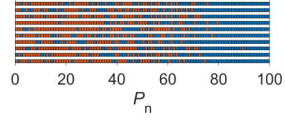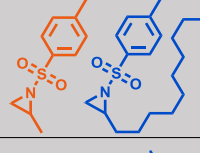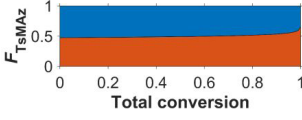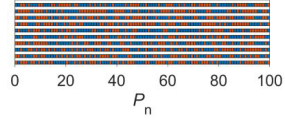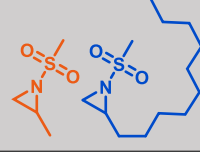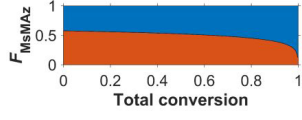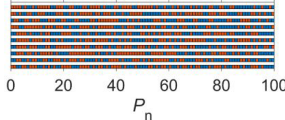
Figure 5. Copolymerization data for the combination of monomers 2 and 7. (A) Monomer concentration as a function of total conversion; (B) logarithmic plot of monomer consumption over time (linearity proves living character); (C) Jaacks fit on in situ NMR data of the copolymerization; (D) BSL fit on in situ NMR data of the copolymerization; (E) Frey fit on in situ NMR data of the copolymerization; and (F) Meyer−Lowry fit on in situ NMR data of the copolymerization. All methods used data from 0 to 50% conversion to determine reactivity values.

The authors also pointed out the importance of choosing the right method to distinguish between nonterminal and terminal copolymerizations to determine accurate reactivity ratios.[62] Nonterminal models like BSL should be preferred for the oxyanionic ring-opening polymerization.[32,33] In addition to the existing nonterminal methods, the authors introduced a method to calculate reactivity ratios based on a simplified version of the Meyer−Lowry equation. The original Meyer−Lowry approach fits both reactivity ratios, while the adapted version fits only one and calculates the other from the reciprocal of r_1 (see eqs 5 and 6). This fitting plot has the same axis as the Meyer−Lowry method (an integrated form of Mayo−Lewis), which allows the direct comparison of nonterminal with a terminal model[32] In 1972, Jaacks reported an elegant method, which does not use the Meyer−Lowry equation to extract reactivity ratios. His approximate terminal model is also applicable to copolymerizations like the one of styrene and methacrylate, which require a terminal model.[36]

In contrast to most literature, in which typically only a single calculation method is used, which might lead to inaccurate results, we used four models to calculate the reactivity ratios for our copolymerizations. We monitored all copolymerizations by in situ ^{1}H NMR and extracted the monomer conversions by selecting one or more distinct proton resonances. To calculate the reactivity ratios, we applied different methods on the data (varying the conversions to minimize the difference of the obtained values). Therefore, we calculated the respective reactivity ratios by the different methods at different conversions (usually up to 40%) to minimize the difference of the resulting reactivity ratios by the linear least-square method (data, which was not used to determine the fit function, is illustrated in gray in the plots in the Supporting Information or Figure 5). In most cases, at least three methods resulted in very similar reactivity ratios (Tables 2 and 3), which also correlate with the reactivity of each monomer expected from the electron-withdrawing effects of the sulfonamide activating groups. To the best of our

Table 2. Comonomer Reactivity and Distributions for Copolymerizations of Sulfonyl Aziridines with Different Activating Groups and the Reactivity Ratios Calculated with Nonterminal Models from Jaacks,[36] Frey,[32] BSL,[33,62] and Meyer–Lowry[34] (M–L). Visualization of the copolymer compositions calculated from the reactivity ratios and via Monte Carlo simulated microstructure of the copolymers[a]

Co-Monomers	Reactivity ratios		Illustrations of microstructures	
	r_1	r_2	Monomer fraction F plotted against total conversion	Monte Carlo simulation of comonomer distribution
	Jaacks	5.476, 0.182		
	Frey	5.526, 0.180		
	BSL	5.540, 0.181		
	M-L	5.634, 0.190		
	Jaacks	5.508, 0.181		
	Frey	5.493, 0.182		
	BSL	5.487, 0.182		
	M-L	5.461, 0.178		
	Jaacks	0.929, 1.074		
	Frey	0.900, 1.110		
	BSL	0.903, 1.106		
	M-L	n. c.		
	Jaacks	1.354, 0.737		
	Frey	1.359, 0.735		
	BSL	1.359, 0.735		
	M-L	1.428, 0.784		

[a]n. c. not calculated. M–L did not give reasonable reactivity ratios for the fitted data with any monomer conversion.

knowledge, this calculation and optimization of reactivity ratios by different methods and varying conversion was not reported before. The electron-withdrawing effects of the sulfonamides, i.e., the electrophilicity of each comonomer, allow the prediction of the expected reactivity ratios and are an additional control over the calculated values. To visualize the polymer microstructures, we used the reactivity ratios based on the method reported recently (Tables 2 and 3),[32] using the equation for comonomer composition (F_1).

$$F_1 = \frac{d[M_1]}{d[M_1] + d[M_2]} = \frac{r_1 f_1^2 + f_1 f_1^2}{r_1 f_1^2 + 2 f_1 f_2 + r_2 f_2^2} \quad (17)$$
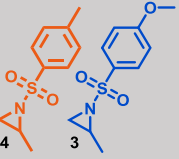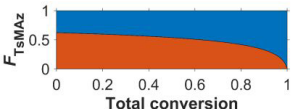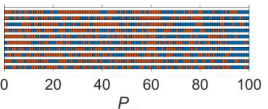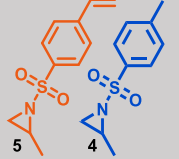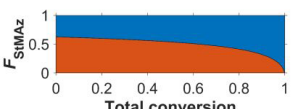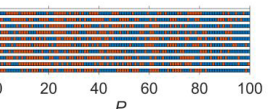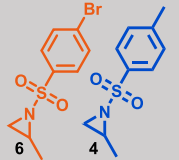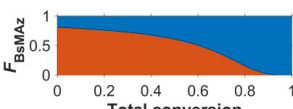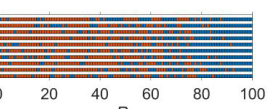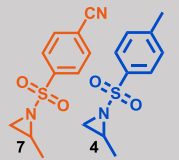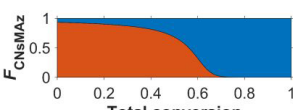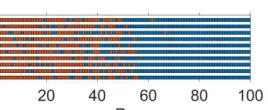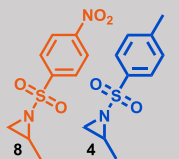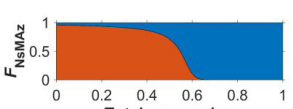
We present two visual illustrations of the monomer distribution in the copolymers: the monomer fraction (F) was plotted against the total conversion for a theoretical 50:50 mixture of both comonomers. This plot easily allows predicting the copolymer microstructure visualizing the gradient strength (Tables 2 and 3, middle plot). In addition, we performed Monte Carlo simulations to visualize the comonomer incorporation. We used the monomer reactivities and plotted a theoretical monomer distribution of 10 individual copolymer chains vs. the degree of polymerization. In contrast to previous visualizations for comonomer sequence distributions calculated by Monte Carlo simulations,[32] we set the molar mass dispersity to unity to exclude chain length effects on the visualization. Both plots allow estimating the percentage of the tapered part in the polymer and the actual gradient strength. Table 2 shows the copolymer compositions of tosyl- and mesyl-activated aziridines with varying side chains. This set of copolymeriza-

tions underlines that the monomer reactivity is dominated by the electron-withdrawing effect of the activation group, while the side gr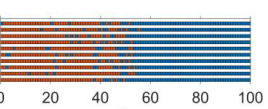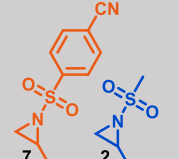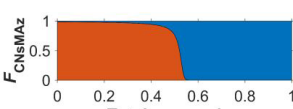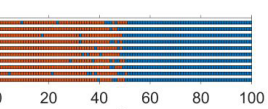oup in the 2-position of the aziridines had only little influence on the comonomer reactivity in those cases. If tosyl monomers were copolymerized with mesyl-activated aziridine (Table 2, entries 1 and 2), copolymers with a medium gradient strength were obtained. No significant difference for the reactivity ratios ($r_1 \approx 5$ and $r_2 \approx 0.2$) and microstructures was determined in both cases. In contrast, for the copolymerization of aziridines with the same activation groups, random copolymers were obtained (entries 3 and 4 of Table 2).

Besides these random and medium gradients (region b in Figure 1), activated aziridines allowed the preparation of other gradient profiles as well. Copolymers with soft gradients were accessible, for example, when (**3**) and (**4**) with reactivity ratios of 1.75 and 0.57 were copolymerized. The gradient with **5** also represented a copolymer with a soft gradient with similar reactivity ratios. We suggest defining a soft gradient for reactivity ratios of r_1: ≤ 2 and r_2: ≥ 0.5.

Increasing the slope of the tapered block further leads to medium gradient copolymers (region b in Figure 1). During the final stages of the copolymerization exclusively to the less reactive monomers is reacting and building a separated block (cf. Table 2, entries 1 and 2). The properties of copolymers with a medium gradient microstructure differ measurably from random copolymers. Copolymers with medium gradients had been reported as compatibilizers in polymer blends, which decreased domain size significantly when compared to block copolymers.[14,21,63,64]

Table 3. Comonomer Reactivity and Distributions for Copolymerizations of Sulfonyl Aziridines of Monomers with Different Activating Groups and the Reactivity Parameters Calculated with Nonterminal Models from Jaacks,[36] Frey,[32] BSL,[33,62] and Meyer−Lowry[34] (M−L). Visualization of the copolymer compositions calculated from the reactivity ratios and via Monte Carlo simulated microstructure of the copolymers[a]

Co-Monomers	Reactivity ratios		Visualization of copolymer microstructures	
	Method	r_1, r_2	Monomer Fraction F plotted against total conversion	Monte Carlo simulation of comonomer distribution
4 **3**	Jaacks	1.674, 0.596		
	Frey	1.752, 0.570		
	BSL	1.759, 0.573		
	M-L	n. c.		
5 **4**	Jaacks	1.681, 0.590		
	Frey	1.682, 0.594		
	BSL	1.675, 0.590		
	M-L	1.477, 0.495		
6 **4**	Jaacks	4.245, 0.235		
	Frey	4.245, 0.235		
	BSL	4.245, 0.235		
	M-L	4.251, 0.236		
7 **4**	Jaacks	13.791, 0.072		
	Frey	14.021, 0.071		
	BSL	14.084, 0.071		
	M-L	17.625, 0.199		
8 **4**	Jaacks	22.664, 0.044		
	Frey	23.347, 0.042		
	BSL	23.801, 0.043		
	M-L	28.880, 0.132		
7 **2**	Jaacks	68.997, 0.014		
	Frey	76.306, 0.013		
	BSL	99.825, 0.013		
	M-L	87.036, 0,027		

[a]n. c. not calculated. M−L did not give reasonable reactivity ratios for the fitted data with any monomer conversion.

As (**6**) has a stronger EWD group, it generated, like MsMAz (**2**) with TsMAz (**4**), a more pronounced gradient yielding a polymer exclusively consisting of the less active monomer (**4**) in the terminal 10%, which is illustrated by the Monte Carlo simulation and the monomer fraction plot. Other soft gradient copolymers were reported for the carbanionic copolymerization of isoprene with myrcene.[56] Reactivity ratios of r_1: 4.4 and r_2: 0.23 formed a soft gradient with a smoothly increasing concentration of isoprene over the total conversion toward a novel bio-based natural rubber. The cationic polymerization also gives examples for the formation of gradients; oxazolines, for example, are known to form soft to medium gradient copolymers, depending on either on steric hindrance or electron pushing or withdrawing behavior of the oxazoline side group.[65,66]

Further increase of slope of the tapered microstructure led to polymers, which can be seen as "triblock" copolymers consisting of a monomer "A" block at the beginning and a monomer "B" block at the end, connected by a mixed block composed of A and B, as illustrated in the green region c in Figure 1.[13,67] Due to the tapered middle block, the chemical interface is smoothed out, which had been detected by electron microscopy.[64,68] We suggest using the term hard gradient copolymer, whenever the structure for a triblock copolymer is clearly visible. Reactivity ratios leading to hard gradients are typically in the order of around r_1: 7.5−25 and r_2: 0.13−0.04. Such hard gradient copolymers were obtained in poly(7-co-4) and poly(8-co-4) (entries 4 and 5, Table 3), proving that ca. 30−40% of the terminal blocks consist exclusively of the monomer with the lower reactivity. The "middle block"

exhibits a hard gradient and spans over 20−30% of the total degree of polymerization.

If the reactivity ratio difference further increases, the gradient profile in this middle block gets even harder and a block-like copolymer is obtained, which is probably not to distinguish from a "real" block copolymer, prepared by sequential monomer addition. In the aziridine family, such block copolymers can be obtained by a competitive copolymerization of a highly activated (**7**) and a less activated monomer (**2**) (entry 6 in Table 3). Poly(**7**-*co*-**2**) copolymers proved a tapered middle segment of only 5% and reactivity ratios of $r_1 = 76.31$ and $r_2 = 0.01$. A further increase in reactivity differences was achieved in a previous study by our group when sulfonyl aziridines were copolymerized with ethylene oxide. This comonomer mixture produced block copolymers with the largest difference in comonomer reactivity reported for anionic polymerization to date ($r_1 = 151$, $r_2 = 0.013$ (**2** and EO) and $r_1 = 265$, $r_2 = 0.004$ (**3** and EO)).

Grune et al. recently conducted copolymerization studies of 4-methylstyrene and isoprene and observed the formation of a hard gradient copolymer with a tapered section of around 10% for reactivity ratios of r_1: 25.4 and r_2: 0.0007.[55] Carbanionic copolymerization of the rapid polymerizing myrcene with styrene showed to give a hard gradient copolymer.[56] Reactivity ratios of r_1: 36 and r_2: 0.028 formed a block polymer with a tapered section of less than 10% (hard gradient), while the copolymerization of myrcene with an even less reactive partner (4-methylstyrene) formed a block copolymer without visible tapering effect (r_1: 140, r_2: 0.0074).[56] To form block-like copolymers according to a one-step polymerization on a monomer mixture, reactivity ratios of $r_1 \geq 20$ and $r_2 \leq 0.02$ are required. An actual difference in the polymer microstructure is not visible if reactivity ratios become extremer than r_1: ∼100 and r_2: ∼0.01. Figure 6 illustrates the effect of the increasing
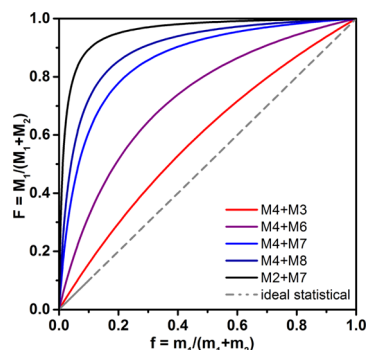

Figure 6. Copolymerization diagram of different comonomer pairs (reactivity ratios are listed in Table 3).

reactivity difference of the comonomer set plotted as a copolymerization diagram (the gray dashed line shows an ideal statistical copolymerization; at any time, the monomer ratios in the solution are similar to the monomer content in the polymer). With an increasing reactivity difference between the monomers, the curves deviate further from the ideal statistical copolymerization, i.e., the more reactive monomer is converted into the polymer faster than the less reactive one.

CONCLUSIONS

Gradient copolymers further expand the properties of copolymers in polymer science. Adjusting the gradient strength by the chemical design of the comonomer reactivity gives access to a variety of new copolymer structures. The family of sulfonyl-activated aziridines was used to prepare a series of gradient copolymers with an adjustable gradient profile, by adjusting the electron-withdrawing effect of the sulfonyl group. The determination of the reactivity ratios of all copolymerizations was conducted by four different methods. The similarity of the results proves that the AROP of aziridines can be described with terminal and nonterminal models. The comonomer library used herein further allowed the prediction of the comonomer reactivity of other activated aziridines and will result in the preparation of even more gradient structures with the potential to be used as compatibilizers or polyelectrolytes after the removal of the activating group.

ASSOCIATED CONTENT

Ⓢ Supporting Information

The Supporting Information is available free of charge at https://pubs.acs.org/doi/10.1021/acs.macromol.9b01623.

> Additional data for monomer preparation and characterization, polymer molar mass data and calculations for reactivity ratios (PDF)

AUTHOR INFORMATION

Corresponding Author
*E-mail: wurm@mpip-mainz.mpg.de.

ORCID
Frederik R. Wurm: 0000-0002-6955-8489

Notes
The authors declare no competing financial interest.

ACKNOWLEDGMENTS

REFERENCES

(1) Roy, R. K.; Meszynska, A.; Laure, C.; Charles, L.; Verchin, C.; Lutz, J.-F. Design and synthesis of digitally encoded polymers that can be decoded and erased. *Nat. Commun,* **2015**, *6*, No. 7237.

(2) Zamfir, M.; Lutz, J.-F. Ultra-precise insertion of functional monomers in chain-growth polymerizations. *Nat. Commun,* **2012**, *3*, No. 1138.

(3) Shen, M.; Bever, M. Gradients in polymeric materials. *J. Mater. Sci.* **1972**, *7*, 741−746.

(4) Kokkinis, D.; Bouville, F.; Studart, A. R. 3D printing of materials with tunable failure via bioinspired mechanical gradients. *Adv. Mater.* **2018**, *30*, No. 1705808.

(5) Claussen, K. U.; Scheibel, T.; Schmidt, H.-W.; Giesa, R. Polymer Gradient Materials: Can Nature Teach Us New Tricks? *Macromol. Mater. Eng.* **2012**, *297*, 938−957.

(6) Cai, H.; Gabryelczyk, B.; Manimekalai, M. S. S.; Gruber, G.; Salentinig, S.; Miserez, A. Self-coacervation of modular squid beak proteins - a comparative study. *Soft Matter* **2017**, *13*, 7740−7752.

(7) Tan, Y.; Hoon, S.; Guerette, P. A.; Wei, W.; Ghadban, A.; Hao, C.; Miserez, A.; Waite, J. H. Infiltration of chitin by protein

coacervates defines the squid beak mechanical gradient. *Nat. Chem. Biol.* **2015**, *11*, 488−495.

(8) Harrington, M. J.; Waite, J. H. How Nature Modulates a Fiber's Mechanical Properties: Mechanically Distinct Fibers Drawn from Natural Mesogenic Block Copolymer Variants. *Adv. Mater.* **2009**, *21*, 440−444.

(9) Alam, M. M.; Jack, K. S.; Hill, D. J. T.; Whittaker, A. K.; Peng, H. Gradient copolymers−Preparation, properties and practice. *Eur. Polym. J.* **2019**, *116*, 394−414.

(10) Zheng, C. Gradient copolymer micelles: an introduction to structures as well as structural transitions. *Soft Matter* **2019**, *15*, 5357−5370.

(11) Thomopoulos, S.; Birman, V.; Genin, G. M. *Structural Interfaces and Attachments in Biology*; Springer-Verlag: New York, 2013.

(12) Knoll, K.; Niessner, N. *Styroflex: A New Transparent Styrene-Butadiene Copolymer with High Flexibility Synthesis, Applications, and Synergism with Other Styrene Polymers*; ACS Symposium Series; American Chemical Society, 1998; pp 112−128.

(13) Ruzette, A.-V.; Leibler, L. Block copolymers in tomorrow's plastics. *Nat. Mater.* **2005**, *4*, 19.

(14) Matyjaszewski, K.; Tsarevsky, N. V. Nanostructured functional materials prepared by atom transfer radical polymerization. *Nat. Chem.* **2009**, *1*, 276.

(15) Lutz, J.-F. *Sequence-Controlled Polymers*; John Wiley & Sons, 2018.

(16) Ouchi, M.; Sawamoto, M. Sequence-controlled polymers via reversible-deactivation radical polymerization. *Polym. J.* **2018**, *50*, 83.

(17) D'Hooge, D.; Van Steenberge, P.; Reyniers, M.-F.; Marin, G. Fed-Batch Control and Visualization of Monomer Sequences of Individual ICAR ATRP Gradient Copolymer Chains. *Polymers* **2014**, *6*, 1074−1095.

(18) Van Steenberge, P. H. M.; D'hooge, D. R.; Wang, Y.; Zhong, M.; Reyniers, M.-F.; Konkolewicz, D.; Matyjaszewski, K.; Marin, G. B. Linear Gradient Quality of ATRP Copolymers. *Macromolecules* **2012**, *45*, 8519−8531.

(19) Gleede, T.; Reisman, L.; Rieger, E.; Mbarushimana, P. C.; Rupar, P. A.; Wurm, F. R. Aziridines and azetidines: building blocks for polyamines by anionic and cationic ring-opening polymerization. *Polym. Chem.* **2019**, *10*, 3257−3283.

(20) Rieger, E.; Alkan, A.; Manhart, A.; Wagner, M.; Wurm, F. R. Sequence-Controlled Polymers via Simultaneous Living Anionic Copolymerization of Competing Monomers. *Macromol. Rapid Commun.* **2016**, *37*, 833−839.

(21) Ganesan, V.; Kumar, N. A.; Pryamitsyn, V. Blockiness and Sequence Polydispersity Effects on the Phase Behavior and Interfacial Properties of Gradient Copolymers. *Macromolecules* **2012**, *45*, 6281−6297.

(22) Reisman, L.; Mbarushimana, C. P.; Cassidy, S. J.; Rupar, P. A. Living Anionic Copolymerization of 1-(Alkylsulfonyl)aziridines to Form Poly(sulfonylaziridine) and Linear Poly(ethylenimine). *ACS Macro Lett.* **2016**, *5*, 1137−1140.

(23) Rieger, E.; Gleede, T.; Manhart, A.; Lamla, M.; Wurm, F. R. Microwave-Assisted Desulfonylation of Polysulfonamides toward Polypropylenimine. *ACS Macro Lett.* **2018**, 598−603.

(24) Gleede, T.; Rieger, E.; Blankenburg, J.; Klein, K.; Wurm, F. R. Fast Access to Amphiphilic Multiblock Architectures by the Anionic Copolymerization of Aziridines and Ethylene Oxide. *J. Am. Chem. Soc.* **2018**, *140*, 13407−13412.

(25) Fierens, S. K.; Van Steenberge, P. H. M.; Reyniers, M. F.; D'Hooge, D. R.; Marin, G. B. Analytical and advanced kinetic models for characterization of chain-growth copolymerization: the state-of-the-art. *React. Chem. Eng.* **2018**, *3*, 128−145.

(26) Rieger, E.; Alkan, A.; Manhart, A.; Wagner, M.; Wurm, F. R. Sequence-Controlled Polymers via Simultaneous Living Anionic Copolymerization of Competing Monomers. *Macromol. Rapid Commun.* **2016**, *37*, 833−839.

(27) Thomi, L.; Wurm, F. R. Living Anionic Polymerization of Functional Aziridines. *Macromol. Symp.* **2015**, *349*, 51−56.

(28) Rieger, E.; Blankenburg, J.; Grune, E.; Wagner, M.; Landfester, K.; Wurm, F. R. Controlling the polymer microstructure in anionic polymerization by compartmentalization. *Angew. Chem., Int. Ed. Engl.* **2018**, *57*, 2483−2487.

(29) Gleede, T.; Rieger, E.; Homann-Müller, T.; Wurm, F. R. 4-Styrenesulfonyl-(2-methyl)aziridine: The First Bivalent Aziridine-Monomer for Anionic and Radical Polymerization. *Macromol. Chem. Phys.* **2018**, No. 1700145.

(30) Freeman, R.; Hill, H. D. W.; Kaptein, R. Proton-Decoupled NMR Spectra of Carbon-13 With the Nuclear Overhauser Effect Suppressed. *J. Magn. Reson.* **1972**, *7*, 327−329.

(31) Wall, F. T. The structure of vinyl copolymers. *J. Am. Chem. Soc.* **1941**, *63*, 1862−1866.

(32) Blankenburg, J.; Kersten, E.; Maciol, K.; Wagner, M.; Zarbakhsh, S.; Frey, H. The poly(propylene oxide-co-ethylene oxide) gradient is controlled by the polymerization method: determination of reactivity ratios by direct comparison of different copolymerization models. *Polym. Chem.* **2019**, *10*, 2863−2871.

(33) Beckingham, B. S.; Sanoja, G. E.; Lynd, N. A. Simple and Accurate Determination of Reactivity Ratios Using a Nonterminal Model of Chain Copolymerization. *Macromolecules* **2015**, *48*, 6922−6930.

(34) Meyer, V. E.; Lowry, G. G. Integral and differential binary copolymerization equations. *J. Polym. Sci., Part A: Gen. Pap.* **1965**, *3*, 2843−2851.

(35) Gleede, T.; Rieger, E.; Liu, L.; Bakkali-Hassani, C.; Wagner, M.; Carlotti, S.; Taton, D.; Andrienko, D.; Wurm, F. R. Alcohol- and Water-Tolerant Living Anionic Polymerization of Aziridines. *Macromolecules* **2018**, *51*, 5713−5719.

(36) Jaacks, V. A novel method of determination of reactivity ratios in binary and ternary copolymerizations. *Macromol. Chem. Phys.* **1972**, *161*, 161−172.

(37) Frisch, M.; Trucks, G.; Schlegel, H.; Scuseria, G.; Robb, M.; Cheeseman, J.; Scalmani, G.; Barone, V.; Mennucci, B.; Petersson, G.. *Gaussian 09*, revision D.01; Gaussian, Inc.: Wallingford CT, 2009.

(38) Becke, A. D. Density-functional thermochemistry. III. The role of exact exchange. *J. Chem. Phys.* **1993**, *98*, 5648−5652.

(39) Clark, T.; Chandrasekhar, J.; Spitznagel, G. W.; Schleyer, P. V. R. Efficient diffuse function-augmented basis sets for anion calculations. III. The 3-21+ G basis set for first-row elements, Li−F. *J. Comput.Chem.* **1983**, *4*, 294−301.

(40) Ditchfield, R.; Hehre, W. J.; Pople, J. A. Self-consistent molecular-orbital methods. IX. An extended Gaussian-type basis for molecular-orbital studies of organic molecules. *J. Chem. Phys.* **1971**, *54*, 724−728.

(41) McLean, A.; Chandler, G. Contracted Gaussian basis sets for molecular calculations. I. Second row atoms, Z= 11−18. *J. Chem. Phys.* **1980**, *72*, 5639−5648.

(42) Miertuš, S.; Scrocco, E.; Tomasi, J. Electrostatic interaction of a solute with a continuum. A direct utilizaion of AB initio molecular potentials for the prevision of solvent effects. *Chem. Phys.* **1981**, *55*, 117−129.

(43) Miertus, S.; Tomasi, J. Approximate evaluations of the electrostatic free energy and internal energy changes in solution processes. *Chem. Phys.* **1982**, *65*, 239−245.

(44) Pascual-ahuir, J.-L.; Silla, E.; Tunon, I. GEPOL: An improved description of molecular surfaces. III. A new algorithm for the computation of a solvent-excluding surface. *J. Comput. Chem.* **1994**, *15*, 1127−1138.

(45) Foster, J.; Weinhold, F. Natural hybrid orbitals. *J. Am. Chem. Soc.* **1980**, *102*, 7211−7218.

(46) Stewart, I. C.; Lee, C. C.; Bergman, R. G.; Toste, F. D. Living ring-opening polymerization of N-sulfonylaziridines: synthesis of high molecular weight linear polyamines. *J. Am. Chem. Soc.* **2005**, *127*, 17616−17617.

(47) Rieger, E.; Manhart, A.; Wurm, F. R. Multihydroxy Polyamines by Living Anionic Polymerization of Aziridines. *ACS Macro Lett.* **2016**, *5*, 195−198.

(48) Rieger, E.; Gleede, T.; Weber, K.; Manhart, A.; Wagner, M.; Wurm, F. R. The living anionic polymerization of activated aziridines: a systematic study of reaction conditions and kinetics. *Polym. Chem.* **2017**, *8*, 2824−2832.

(49) Mbarushimana, P. C.; Liang, Q.; Allred, J. M.; Rupar, P. A. Polymerizations of Nitrophenylsulfonyl-Activated Aziridines. *Macromolecules* **2018**, *51*, 977−983.

(50) Ishizone, T.; Hirao, A.; Nakahama, S. Anionic Polymerization of Monomers Containing Functional Groups. 6. Anionic Block Copolymerization of Styrene Derivatives Para-Substituted with Electron-Withdrawing Groups. *Macromolecules* **1993**, *26*, 6964−6975.

(51) Hansch, C.; Leo, A.; Taft, R. W. A Survey of Hammett Substituent Constants and Resonance and Field Parameters. *Chem. Rev.* **1991**, *91*, 165−195.

(52) Stanetty, C.; Blaukopf, M. K.; Lachmann, B.; Noe, C. R. The Dinosyl Group: A Powerful Activator for the Regioselective Alcoholysis of Aziridines. *Eur. J. Org. Chem.* **2011**, *2011*, 3126−3130.

(53) Sedlacek, O.; Lava, K.; Verbraeken, B.; Kasmi, S.; De Geest, B. G.; Hoogenboom, R. Unexpected Reactivity Switch in the Statistical Copolymerization of 2-Oxazolines and 2-Oxazines Enabling the One-Step Synthesis of Amphiphilic Gradient Copolymers. *J. Am. Chem. Soc.* **2019**, *141*, 9617−9622.

(54) Van Steenberge, P. H. M.; Sedlacek, O.; Hernandez-Ortiz, J. C.; Verbraeken, B.; Reyniers, M. F.; Hoogenboom, R.; D'Hooge D, R. Visualization and design of the functional group distribution during statistical copolymerization. *Nat. Commun.* **2019**, *10*, No. 3641.

(55) Grune, E.; Johann, T.; Appold, M.; Wahlen, C.; Blankenburg, J.; Leibig, D.; Müller, A. H. E.; Gallei, M.; Frey, H. One-Step Block Copolymer Synthesis versus Sequential Monomer Addition: A Fundamental Study Reveals That One Methyl Group Makes a Difference. *Macromolecules* **2018**, *51*, 3527−3537.

(56) Grune, E.; Bareuther, J.; Blankenburg, J.; Appold, M.; Shaw, L.; Müller, A. H. E.; Floudas, G.; Hutchings, L. R.; Gallei, M.; Frey, H. Towards bio-based tapered block copolymers: the behaviour of myrcene in the statistical anionic copolymerisation. *Polym. Chem.* **2019**, *10*, 1213−1220.

(57) Grune, E.; Appold, M.; Müller, A. H. E.; Gallei, M.; Frey, H. Anionic Copolymerization Enables the Scalable Synthesis of Alternating (AB)n Multiblock Copolymers with High Molecular Weight in n/2 Steps. *ACS Macro Lett.* **2018**, 807−810.

(58) Herzberger, J.; Leibig, D.; Liermann, J. C.; Frey, H. Conventional Oxyanionic versus Monomer-Activated Anionic Co-polymerization of Ethylene Oxide with Glycidyl Ethers: Striking Differences in Reactivity Ratios. *ACS Macro Lett.* **2016**, *5*, 1206−1211.

(59) Alfrey, T., Jr.; Goldfinger, G. The mechanism of copolymerization. *J. Chem. Phys.* **1944**, *12*, 205−209.

(60) Mayo, F. R.; Lewis, F. M. Copolymerization. I. A basis for comparing the behavior of monomers in copolymerization; the copolymerization of styrene and methyl methacrylate. *J. Am. Chem. Soc.* **1944**, *66*, 1594−1601.

(61) D'hooge, D. R.; Van Steenberge, P. H.; Derboven, P.; Reyniers, M.-F.; Marin, G. B. Model-based design of the polymer micro-structure: bridging the gap between polymer chemistry and engineering. *Polym. Chem.* **2015**, *6*, 7081−7096.

(62) Lynd, N. A.; Ferrier, R. C.; Beckingham, B. S. Recommendation for Accurate Experimental Determination of Reactivity Ratios in Chain Copolymerization. *Macromolecules* **2019**, *52*, 2277−2285.

(63) Malik, R.; Hall, C. K.; Genzer, J. Effect of copolymer compatibilizer sequence on the dynamics of phase separation of immiscible binary homopolymer blends. *Soft Matter* **2011**, *7*, 10620.

(64) Mok, M. M.; Torkelson, J. M. Imaging of phase segregation in gradient copolymers: Island and hole surface topography. *Journal of Polymer Science Part B: Polymer Physics* **2012**, *50*, 189−197.

(65) Verbraeken, B.; Monnery, B. D.; Lava, K.; Hoogenboom, R. The chemistry of poly(2-oxazoline)s. *Eur. Polym. J.* **2017**, *88*, 451−469.

(66) Hoogenboom, R.; Lambermont-Thijs, H. M. L.; Jochems, M. J. H. C.; Hoeppener, S.; Guerlain, C.; Fustin, C.-A.; Gohy, J.-F.; Schubert, U. S. A schizophrenic gradient copolymer: switching and reversing poly(2-oxazoline) micelles based on UCST and subtle solvent changes. *Soft Matter* **2009**, *5*, 3590−3592.

(67) Kryszewski, M. Gradient polymers and copolymers. *Polym. Adv. Technol.* **1998**, *9*, 244−259.

(68) Singh, N.; Tureau, M. S.; Epps, T. H., III Manipulating ordering transitions in interfacially modified block copolymers. *Soft Matter* **2009**, *5*, 4757.